Journal of Non-Crystalline Solids 378 (2013) 163–167

Contents lists available at ScienceDirect

Journal of Non-Crystalline Solids

journal homepage: www.elsevier.com/ locate/ jnoncrysol

Structural rationalization of the microhardness trends of rare-earth aluminosilicate glasses: Interplay between the RE^{3+} field-strength and the aluminum coordinations

Baltzar Stevensson, Mattias Edén *

Physical Chemistry Division, Department of Materials and Environmental Chemistry, Arrhenius Laboratory, Stockholm University, SE-106 91 Stockholm, Sweden

ARTICLE INFO

Article history:
Received 22 April 2013
Received in revised form 11 June 2013
Available online 24 July 2013

Keywords:
RE_2O_3–Al_2O_3–SiO_2 glass;
Microhardness;
Aluminum coordinations;
Structure–property relationships;
Oxynitride glass

ABSTRACT

Many studies have sought to rationalize property/structure relationships in rare-earth (RE) bearing aluminosilicate oxide or oxynitride glasses. In a set of 48 RE_2O_3–Al_2O_3–SiO_2 (RE = La, Y, Lu, Sc) glasses of widely spanning compositions and RE^{3+} cation field-strengths (CFS), we observe strong correlations between the microhardness, glass compactness, and the average coordination number of Al. We argue that the well-known microhardness elevation for increasing RE^{3+} CFS stems not primarily from the RE^{3+} ions themselves, as hitherto believed, but merely from a structure-strengthening by AlO_5/AlO_6 polyhedra that cross-link different glass–network segments. The high-coordination Al populations grow together with the RE^{3+} CFS.

1. Introduction

The chemical inertness of rare-earth RE_2O_3–Al_2O_3–SiO_2 glasses coupled with their advantageous mechanical (*e.g.*, high microhardness and elastic modulus) and optical (high refractive index) properties [1–5], has rendered them valuable in several application areas. Further, research targeting composition–property relations of amorphous RE–(Al)–Si–O–N *oxynitride* phases [6–14] originate from their presence as intergranular components in Si_3N_4-based ceramics, whose properties are strongly affected by the sintering–deriving glasses.

It is well-established that many physical features of RE–Al–Si–O–(N) glasses correlate with the RE^{3+} cation field-strength (CFS) [3–7,11–18] that is given by the square of the charge (z) of the ion divided by its radius (r_{RE}): z/r_{RE}^2. For a given RE aluminosilicate (AS) glass composition, both the glass transition temperature (T_g) and Vickers hardness (H_V) generally elevate for increasing RE^{3+} CFS [3–7,11–17], but the insight into the underlying *structural* reasons is very limited. The microhardness of a silicate-based glass is dictated by several factors [4,11,12,18–21], such as the cation–oxygen bond-strengths, the fractional compactness (C; ion-packing density), and the polymerization/topology of the network of interconnected SiO_4 and AlO_4 tetrahedra. Despite that the RE^{3+} ions depolymerize the network by converting bridging oxygen (BO) into non-bridging oxygen (NBO) species [10,15–17,22–24], and that the microhardness generally diminishes for increasing alkali or alkaline-earth ion content in both oxide [20] and oxynitride glasses [25] (as expected), it merely *grows* together with the RE^{3+} content [14–18,26].

Current rationalizations of the observed boosts of the microhardness and elastic modulus for increasing CFS (major effect) or RE^{3+} content (minor) involve (*i*) the relatively strong RE^{3+}–O bonds compared to those of lower field-strength mono- or di-valent cations [3–5,11–14,17,18,26] and (*ii*) a structural strengthening stemming from the cross-linking of various network fragments by the REO_p polyhedra [2,5,12]. Recently, we proposed an alternative explanation for the microhardness trends of RE_2O_3–Al_2O_3–SiO_2 glasses based on Y and Lu [16], which involves both bond-strength and network cross-linking effects: however, while *originating* from the high CFS of the RE^{3+} ions, the spotlight is rather moved onto the accompanying elevated coordination numbers of the Al species and their associated network cross-linking that we argue is mainly responsible for the enhanced microhardness. The RE^{3+} cations have been suggested to compete with Al^{3+} for lower-coordination sites in the glass structure [5,22,23], thereby inducing significant amounts of AlO_5 and (to a lesser extent) AlO_6 polyhedra, according to schematic equilibria such as [22,23]

$$REO_7 + AlO_4 \rightleftharpoons REO_{7-q} + AlO_{4+q}, \quad q = 1,\ 2. \tag{1}$$

The AlO_5 populations increase markedly together with the RE^{3+} CFS [15–17,22,23]: they range from ≲10% out of the entire {AlO_4, AlO_5, AlO_6} speciation in the La–Al–Si–O system [24] to >30% in its Sc

* Corresponding author. Tel.: +46 8 162375; fax: +46 8 152187.
E-mail address: mattias.eden@mmk.su.se (M. Edén).

0022-3093
http://dx.doi.org/10.1016/j.jnoncrysol.2013.06.013

Table 1
Composition/property/structure data.[a]

RE system	r_{RE} [b] (pm)	Number of samples	$x(RE_2O_3)$	$x(Al_2O_3)$	$x(SiO_2)$	H_V (GPa)	M_V ($cm^3\ mol^{-1}$)	C	$\overline{Z}_{Al}$	$x_{Al}^{[4]}$	$x_{Al}^{[5]}$	$x_{Al}^{[6]}$
La [24,26]	103.2	12	0.11–0.25	0.11–0.30	0.48–0.78	6.28–8.07	8.03–8.56[c]	0.495–0.527[c]	4.04–4.19	0.875–0.949	0.035–0.119	0.005–0.031
Y [16]	90.0	13	0.14–0.25	0.14–0.37	0.42–0.68	7.21–8.92	7.38–7.94	0.519–0.552	4.19–4.32	0.723–0.830	0.153–0.232	0.017–0.045
Lu [16]	86.1	17	0.14–0.24	0.20–0.36	0.49–0.65	8.24–9.15	7.38–7.78	0.529–0.548	4.27–4.36	0.688–0.754	0.225–0.271	0.021–0.043
Sc [17]	74.5	6	0.15–0.21	0.28–0.36	0.49–0.55	9.25–9.45	7.09–7.43	0.541–0.564	4.39–4.46	0.598–0.644	0.301–0.353	0.044–0.054

[a] Observed ranges of glass compositions and experimentally derived values of the Vickers hardness (H_V; uncertainty less than ±0.1 GPa), molar volume (M_V; ±0.02 $cm^3\ mol^{-1}$), fractional compactness (C; ±0.001), ^{27}Al NMR-derived average Al coordination numbers ($\overline{Z}_{Al}$; ≈ ± 0.015) and fractional populations of AlO_p groups ($x_{Al}^{[p]}$; ± 0.015), where ±σ uncertainties are given within parenthesis. The data are reproduced from the as-indicated references.
[b] Shannon-Prewitt [36] RE^{3+} radius (assuming six-fold coordination by oxygen).
[c] Corrected values of those reported by Iftekhar et al. [26].

counterpart [17], whereas the AlO_6 populations display a similar trend but remain ≲5% throughout [17,24].

For RE_2O_3–Al_2O_3–SiO_2 glasses across the Y and Lu systems, we observed a high correlation between the microhardness and the average Al coordination number ($\overline{Z}_{Al}$) [16]. However, given the relatively similar Y^{3+} and Lu^{3+} ionic radii and thereby close CFS-values of 3.7 $Å^{-2}$ and 4.0 $Å^{-2}$, respectively, it is unclear how well this trend remains over a wider CFS range. Herein, we firmly establish the $H_V/\overline{Z}_{Al}$ relationship for 48 glasses from four RE_2O_3–Al_2O_3–SiO_2 systems (RE = La, Y, Lu, Sc) that exhibit a large RE^{3+} CFS-span between 2.8 $Å^{-2}$ (for La^{3+}) and 5.4 $Å^{-2}$ (for Sc^{3+}) and featuring widely varying RE/Al/Si contents that for the Lu and Sc RE AS systems encompass their entire glass-forming regions attainable by a standard melt-quench procedure at 1650 °C [15–17].

2. Experimental procedures

Table 1 lists the ranges of the oxide equivalents and observed values of H_V, C, M_V (molar volume) and $\overline{Z}_{Al}$ for the RE_2O_3–Al_2O_3–SiO_2 glasses. The compositions within each RE system are illustrated in Fig. 1 of Iftekhar et al. [15]. The detailed compositional and structural data, as well as the physical properties, were previously reported for each La [24,26,27], Y [16], Lu [16], and Sc [17] based AS glass, as were all procedures for sample preparations, physical-property measurements, and ^{27}Al nuclear magnetic resonance (NMR) experimentation; here we only recapitulate the most relevant details.

2.1. Glass synthesis and characterization

The glass synthesis protocol is outlined in detail by Iftekhar et al. [15]. High-purity oxide precursors were heated sequentially in Pt crucibles up to final temperatures of 1600 °C (for La and Y based glasses), or 1650 °C (for Lu and Sc). The melts were held for 60 min and quenched by immersing the bottom of the crucible in water. No annealing was performed to avoid any potential alteration of the as-quenched glass structures for our subsequent NMR investigations on local and intermediate-range structures [15–17,24,27]. While annealing may reduce stress in the glasses and thereby affect the microhardness [20], the present work focuses on explaining relative trends among RE-bearing AS glasses that were all handled by identical procedures.

Each sample constitutes a single homogeneous amorphous phase, as confirmed by powder X-ray diffraction and scanning electron microscopy (SEM) in backscatter mode using a JSM 7000F JEOL instrument. SEM coupled with energy-dispersive X-ray spectroscopy (EDS) verified that each composition was close to its batched counterpart. Several specimens were also examined by transmission electron microscopy/EDS, which further confirmed the homogeneity down to a ≲10 nm scale, *i.e.*, within the limits of our instrument (JEM 2100F; JEOL). All physical properties were examined on glass pieces devoid of bubbles.

2.2. Al coordinations

The average coordination number of Al ($\overline{Z}_{Al}$) was determined for each glass by deconvoluting its ^{27}Al NMR spectrum, recorded at 14.1 T and 24.0 kHz magic-angle spinning, into signals from AlO_4, AlO_5 and AlO_6 groups. This provided a set of fractional populations $\{x_{Al}^{[4]}, x_{Al}^{[5]}, x_{Al}^{[6]}\}$, (listed in Table 1) that obey the normalization

$$\sum_p x_{Al}^{[p]} = 1. \tag{2}$$

The numerically exact simulations of the ^{27}Al NMR spectra followed the protocol given in Stevensson et al. [28], while the iterative fitting procedure is described further in Ref. [16]. Besides the fractional populations, the ^{27}Al isotropic chemical shifts and quadrupolar products varied between the iterations, as well as their respective distributions according to Gaussian and Czjzek functionalities [29,30], respectively. Some parameters were constrained within ranges; see Iftekhar et al. [16] for details. The uncertainty of each $x_{Al}^{[p]}$-value is roughly ±0.015 [16,17,24], and was obtained as the range over which each parameter could vary freely, while the root-mean-square deviation between the experiment and simulation remained within ≈20% of its global minimum. Our previous work provides graphical comparisons between the experimental and best-fit NMR spectra [16,17,24].

The $\overline{Z}_{Al}$-value was calculated as the following weighted average:

$$\overline{Z}_{Al} = \sum_p p x_{Al}^{[p]}. \tag{3}$$

The associated uncertainty $[\sigma(\overline{Z}_{Al})]$ is not straightforward to define precisely due to the presence of three contributions ($px_{Al}^{[p]}$) coupled *via* Eq. (2). However, it is conservatively bounded by $0 \le \sigma(\overline{Z}_{Al}) \le \sqrt{2}\sigma\left(x_{Al}^{[p]}\right) = 0.021$. Further, given that $x_{Al}^{[6]}$ is low throughout (≲ 0.05), the uncertainty of $\overline{Z}_{Al}$ is dictated largely by the uncertainties of the two primary $x_{Al}^{[4]}$ and $x_{Al}^{[5]}$ populations: combining Eqs. (2) and (3) then provides the approximate result $\sigma(\overline{Z}_{Al}) \approx \sigma\left(x_{Al}^{[p]}\right) = 0.015$.

2.3. Physical properties

Densities were determined by the Archimedes method in distilled water at 22 °C (ρ = 0.998 gcm^{-3}), from which each molar volume (±0.02 $cm^3\ mol^{-1}$) and fractional compactness (±0.001) were derived: $C = 4\pi N_A/(3M_V)\sum_E x_E r_E^3$, where N_A is Avogadro's constant and x_E denotes the molar fraction of element E in the specimen. The as-assumed coordination numbers $\{Z_{RE} = 6, Z_{Si} = 4, Z_O = 2\}$ were employed together with the experimental $\overline{Z}_{Al}$-value for each glass.

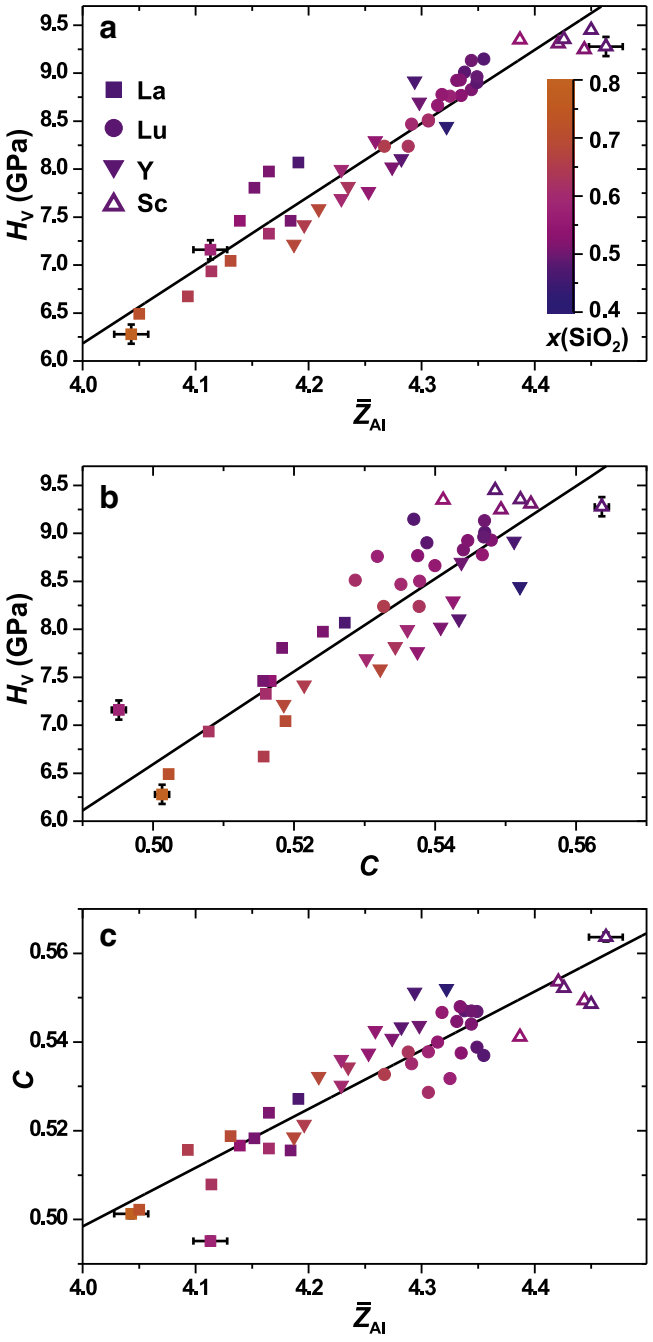

Fig. 1. Property/structure correlations of RE–Al–Si–O glasses for the as-indicated La, Y, Lu, and Sc systems, with best-fit relationships shown by straight lines: (a) H_V against $\overline{Z}_{Al}$ [H_V/GPa = −24(1) + 7.7(3)$\overline{Z}_{Al}$]; (b) H_V against C [H_V/GPa = −18(2) + 48(4) C]; (c) C against $\overline{Z}_{Al}$ [C = −0.03(4) + 0.13(1)$\overline{Z}_{Al}$]. Only a few error-bars are indicated for visual clarity. The color of each symbol reflects the silica content of the glass.

For the microhardness measurements, the glass pieces (≈2–3 mm in diameter) were embedded in thermal plastics as sample holder. Each surface was wet-polished using a 1000 mesh SiC paper. The Vickers hardness was measured (100 g load for 20 s) by a Matsuzawa microhardness tester (MXT-α1) equipped with a pyramidal diamond indenter. The indentations were examined and assessed by SEM in secondary electron mode. No cracks were observed around the indentations. The H_V-values (in GPa) were calculated from the expression $H_V = 1854F/d^2$, where $F = 0.982$ N and d is the average indentation diagonal in μm, according to Anstis et al. [31]. The values are reported as averages over 7–12 independent measurements. The standard deviations vary slightly among the RE systems, but consistently obey $\sigma \leq 0.1$ GPa.

3. Results and discussion

3.1. Relationship between H_V and $\overline{Z}_{Al}$

Fig. 1(a) evidences a strong correlation ($R^2 = 0.92$) between H_V and $\overline{Z}_{Al}$ across the entire set of RE_2O_3–Al_2O_3–SiO_2 glasses; it is readily rationalized by the following structure-based mechanism (Table 2 lists the R^2-values of the fits discussed below):

(*i*) The microhardness is assumed to be controlled primarily by the various cation–oxygen bond-strengths and the polymerization of the structure, reflected both by the glass network connectivity and the cross-linking degree of its various segments [7,11,12,32]. The good correlation between H_V and C observed in Fig. 1(b) justifies this assumption.

(*ii*) The cation–oxygen bond-strengths decrease as $Si^{[4]}-O \gg Al^{[4]}-O > Al^{[5]}-O \gg RE^{[p]}-O$. Despite that the Si–O bonds give the most significant net contributions to H_V in (alumino)silicate glasses, for a fixed SiO_2 content they remain constant and may consequently not account for a dependence of the microhardness on substitutions among distinct modifiers featuring a fixed charge. The $Al^{[5]}-O$ and $Al^{[6]}-O$ links are weaker than their $Si^{[4]}-O$ and $Al^{[4]}-O$ counterparts. However, as opposed to the latter *intra*-network bonds, the AlO_5 and AlO_6 polyhedra may connect *different* network segments, thereby condensing and stiffening the structure to concomitantly enhance H_V [16]: this is corroborated by the direct linear $C/\overline{Z}_{Al}$ relationship established in Fig. 1(c). The same arguments about increased cross-linking effects of AlO_6 groups relative to AlO_4 tetrahedra have been invoked to rationalize observed T_g-elevations in Na–Al–P–O glasses [33]. Further, Zheng et al. [21] recently suggested that $Al^{[5]}$ coordinations could be responsible for an observed H_V-increase in boroaluminosilicate glasses. Owing to the strong correlation between C and M_V, all conclusions herein remain valid, and are even reinforced, if C is replaced by M_V in the numerical fitting (Table 2).

(*iii*) As previously suggested [2,5,12], the REO_p polyhedra may also constitute network cross-linking sites. However, their weaker cation–oxygen bonds should amount in a lower structural strengthening than their $Al^{[p]}-O$ analogs, further exacerbated by the preference of $Al^{[p]}$ and $RE^{[p]}$ to coordinate BO and NBO species, respectively. This intuitive statement was verified by molecular dynamics (MD) simulations [34]. While detailed and

Table 2
Property/structure correlations.[a]

Property	Fitting parameter(s)	R^2		
		All	La/Lu	Y/Sc
H_V	C	**0.77**	0.86	0.71
H_V	M_V	0.78	0.85	0.81
H_V	$\overline{Z}_{Al}$	**0.92**	0.95	0.89
C	$\overline{Z}_{Al}$	**0.82**	0.87	0.68
M_V	$\overline{Z}_{Al}$	0.87	0.88	0.89
C	M_V	0.94	0.95	0.89
H_V	CFS/$x(RE_2O_3)$	0.81	0.88	0.91
C	CFS/$x(RE_2O_3)$	0.68	0.78	0.55
M_V	CFS/$x(RE_2O_3)$	0.74	0.86	0.65

[a] Quality (R^2) of the linear fit of the glass property (listed in the first column) to the parameter A (second column) or pair of parameters A and B (A/B). The expression for R^2 accounts for the number of independent fitting parameters. The fits included either data from all RE–Al–Si–O glass specimens, or solely those from the La/Lu and Y/Sc pairs, respectively. Bold-face entries represent R^2 values for the fits plotted in Fig. 1; note that $\overline{Z}_{Al}$-based correlations are consistently better than those offered by alternative parameter sets, as discussed in Section 3.2.

accurate $RE^{[p]}$ speciations are very difficult to assess experimentally in RE AS glasses, a recent X-ray spectroscopy study reported $\overline{Z}_{RE} = 6 \pm 0.5$ throughout the series of lanthanide cations when each is present at 5 wt-% RE_2O_3 in a $Na_2Si_2O_5$ base glass [35]. Furthermore, MD simulations reveal that REO_6 polyhedra dominate in the present structures (except for ScO_5 in the case of Sc^{3+}), whereas $Lu^{[5]}$, $Sc^{[6]}$, $Y^{[7]}$, and $La^{[7]}$ coordinations represent the second most abundant species of each respective cation [16,24,34]. Noteworthy, the relatively modest average coordination numbers $\overline{Z}_{RE} \approx 6$ are only ≈ 2 units higher than the typical $\overline{Z}_{Al}$-values. Hence, even when disregarding the weaker nature of the RE – O bonds and their lower directionality, the cross-linking capabilities of the REO_p polyhedra ($p = 5, 6, 7$) are not substantially higher than those offered by the AlO_5 groups.

(*iv*) While we argue that the AlO_5 polyhedra primarily account for the enhanced glass compactness and accompanying microhardness boost, we stress that all these effects *originate* from the high RE^{3+} CFS (see Table 1). The very sparse reports on quantitative $Al^{[p]}$ speciations in RE-bearing AS glasses coupled to a sole attribution of physical-property alterations *directly* to the RE^{3+} modifiers are likely the main reasons why the prominent role of the AlO_p species for dictating H_V has hitherto passed unnoticed.

3.2. Further considerations

Unambiguous evidence cannot be provided for our proposed mechanism [(*i*)–(*iii*)], although a similar lack of evidence is equally apparent for the prevailing *assumed* "direct" H_V/RE relationship [2–5,11–14,17,18,26]. Noteworthy, neither H_V nor C reveals nearly as strong correlation with any other composition or structure related parameter as with $\overline{Z}_{Al}$, where we also explored several two-parameter fits based on molar fractions of oxides or cations, including their combinations with the RE^{3+} CFS-values. Table 2 lists some of the best alternatives. Furthermore, the $H_V/\overline{Z}_{Al}$ and $C/\overline{Z}_{Al}$ relationships did not improve significantly by invoking a second independent fitting parameter, *e.g.*, $x(SiO_2)$, $x(Al_2O_3)$ or $x(RE_2O_3)$. Only two-parameter fits involving the CFS and $x(RE_2O_3)$ could reproduce the trends in H_V, C, or M_V reasonably well (Table 2), albeit they are consistently weaker than those offered by $\overline{Z}_{Al}$ alone. The pair of CFS/$x(RE_2O_3)$ parameters represents the simplest "phenomenological" approach to capture the hitherto argued structural strengthening by the RE – O bonds (approximated by the CFS) and the number of cross-linking RE sites [proportional to $x(RE_2O_3)$].

The remaining deviation from a perfect $H_V/\overline{Z}_{Al}$ fit, as well as the relatively minor discrepancies observed between the Sc/Y and lanthanide pairs (see Table 2) are likely related to the following: for a fixed RE–Al–Si–O composition, both H_V and $\overline{Z}_{Al}$ depend foremost on the RE^{3+} CFS (see Table 1), whereas *within* a given RE_2O_3–Al_2O_3–SiO_2 glass family, they reveal slightly different trends [16,24,26]: $\overline{Z}_{Al}$ decreases linearly as $x(SiO_2)$ increases within each system ($0.58 \leq R^2 \leq 0.94$). While H_V also correlates reasonably well with $x(SiO_2)$ within each RE family (except for Sc)—particularly so for those of La ($R^2 = 0.86$) and Lu ($R^2 = 0.90$)—it exhibits the *strongest* correlation with $x(RE_2O_3)$ for the cases of Y and Sc ($R^2 = 0.81$ for each). Consequently, when considering the entire set of glasses, neither H_V nor $\overline{Z}_{Al}$ fits well to any single oxide molar fraction, where no correlation is observed against $x(RE_2O_3)$ and roughly equal weak fits ($R^2 \approx 0.5$) are obtained for $x(SiO_2)$ and $x(Al_2O_3)$.

An apparently weak correlation observed between H_V and $x(Al_2O_3)$ is perhaps surprising. Yet, while the microhardness elevates slightly for decreasing $x(SiO_2)$ [*i.e.*, increasing $x(Al_2O_3) + x(RE_2O_3)$] within each RE AS system [see Fig. 1(a)], the H_V-dependence on the Al content remains intertwined with the RE^{3+} CFS: since the glass-forming region contracts towards SiO_2-poorer and Al_2O_3-richer compositions for growing CFS (see Table 1 herein and Fig. 1 of Iftekhar et al. [15]), the Lu and Sc glasses feature, on the average, higher Al contents than their Y and La counterparts.

Considering RE-bearing oxynitride glasses, their enhanced network polymerization from the $N^{[3]}$ coordinations is believed to primarily dictate the microhardness [6–8,11–13,19]. However, the situation is more complex for glasses rich in both N and RE species [9,10] that display relatively *fragmented* networks [10,26]. Nevertheless, for glasses featuring low/intermediate N contents ($\lesssim 30$ eq-%), the contributions to H_V from N and RE species are shown to be independent and additive [7,13]. Hence, the herein identified structural feature *primarily* governing the microhardness of RE_2O_3–Al_2O_3–SiO_2 glasses is likely also manifested by their oxynitride analogs, although there it should rank second to the contributions from N.

4. Conclusions

We have explored an alternative explanation for the well-known microhardness elevation in RE_2O_3–Al_2O_3–SiO_2 glasses when the RE^{3+} CFS increases. It originates from the concurrent growth of the AlO_5 populations and their enhanced network cross-linking effects through relatively strong $Al^{[5]} - O - T$ bonds ($T = Si^{[4]}$, $Al^{[4]}$). While previously proposed analogous cross-linking contributions from $RE^{[p]}$–O–T structural fragments [2,5,12] likely also contribute to the high H_V-values observed from RE AS glasses, their bearings should be more modest compared to those of the stronger Al – O bonds. Our picture naturally connects two inherent features of RE AS glasses—both being distinctly different to their counterparts involving lower-CFS M^+ or M^{2+} modifier ions—namely that they manifest *both* high H_V-values *and* significant AlO_5 populations. The elastic modulus is possibly also largely governed by structure-strengthening effects from AlO_p polyhedra. This is an interesting line for future investigations, as is the precise relationship between $\overline{Z}_{Al}$ and H_V for oxynitride AS glasses.

Acknowledgments

This work was supported by the Swedish Research Council (contracts VR-NT 2009-7551 and 2010-4943) and the Faculty of Sciences at Stockholm University. We thank Jekabs Grins for discussions.

References

[1] A. Makishima, Y. Tamura, T. Sakaino, J. Am. Ceram. Soc. 61 (1978) 247–249.
[2] S. Tanabe, N. Soga, K. Hirao, T. Hanada, J. Am. Ceram. Soc. 73 (1990) 1733–1736.
[3] J.T. Kohli, J.E. Shelby, Phys. Chem. Glasses 32 (1991) 67–71.
[4] J.T. Kohli, J.E. Shelby, J. Am. Ceram. Soc. 74 (1991) 1031–1035.
[5] S. Tanabe, K. Hirao, N. Soga, J. Am. Ceram. Soc. 75 (1992) 503–506.
[6] M. Ohashi, K. Nakamura, K. Hirao, S. Kanzaki, S. Hampshire, J. Am. Ceram. Soc. 78 (1995) 71–76.
[7] F. Lofaj, R. Statet, M.J. Hoffmann, A.R. de Arellano López, J. Eur. Ceram. Soc. 24 (2004) 3377–3385.
[8] H.-O. Mulfinger, J. Am. Ceram. Soc. 49 (1966) 462–467.
[9] A.S. Hakeem, R. Daucé, E. Leonova, M. Edén, Z. Shen, J. Grins, S. Esmaeilzadeh, Adv. Mater. 17 (2005) 2214–2216.
[10] E. Leonova, A.S. Hakeem, K. Jansson, B. Stevensson, Z. Shen, J. Grins, S. Esmaeilzadeh, M. Edén, J. Non-Cryst. Solids 354 (2008) 49–60.
[11] R. Ramesh, E. Nestor, M.J. Pomeroy, S. Hampshire, J. Eur. Ceram. Soc. 17 (1997) 1933–1939.
[12] P.F. Becher, S.B. Waters, C.G. Westmoreland, L. Riester, J. Am. Ceram. Soc. 85 (2002) 897–902.
[13] M.J. Pomeroy, C. Mulcahy, S. Hampshire, J. Am. Ceram. Soc. 86 (2003) 458–464.
[14] M.J. Pomeroy, E. Nestor, R. Ramesh, S. Hampshire, J. Am. Ceram. Soc. 88 (2005) 875–881.
[15] S. Iftekhar, J. Grins, P.N. Gunawidjaja, M. Edén, J. Am. Ceram. Soc. 94 (2011) 2429–2435.
[16] S. Iftekhar, B. Pahari, K. Okhotnikov, A. Jaworski, B. Stevensson, J. Grins, M. Edén, J. Phys. Chem. C 116 (2012) 18394–18406.
[17] B. Pahari, S. Iftekhar, A. Jaworski, K. Okhotnikov, K. Jansson, B. Stevensson, J. Grins, M. Edén, J. Am. Ceram. Soc. 95 (2012) 2545–2553.
[18] H. Lemercier, T. Rouxel, D. Fargeot, J.-L. Besson, B. Piriou, J. Non-Cryst. Solids 201 (1996) 128–145.
[19] T. Rouxel, J. Am. Ceram. Soc. 90 (2007) 3019–3039.
[20] M.M. Smedskjaer, M. Jensen, Y. Yue, J. Non-Cryst. Solids 356 (2010) 893–897.
[21] Q. Zheng, M. Potuzak, J.C. Mauro, M.M. Smedskjaer, R.E. Youngman, Y. Yue, J. Non-Cryst. Solids 358 (2012) 993–1002.
[22] T. Schaller, J.F. Stebbins, J. Phys. Chem. B 102 (1998) 10690–10697.

[23] P. Florian, N. Sadiki, D. Massiot, J.P. Coutures, J. Phys. Chem. B 111 (2007) 9747–9757.
[24] A. Jaworski, B. Stevensson, B. Pahari, K. Okhotnikov, M. Edén, Phys. Chem. Chem. Phys. 14 (2012) 15866–15878.
[25] S. Ali, B. Jonson, J. Eur. Ceram. Soc. 31 (2011) 611–618.
[26] S. Iftekhar, J. Grins, M. Edén, J. Non-Cryst. Solids 356 (2010) 1043–1048.
[27] S. Iftekhar, E. Leonova, M. Edén, J. Non-Cryst. Solids 355 (2009) 2165–2174.
[28] B. Stevensson, M. Edén, J. Chem. Phys. 134 (2011) 124104.
[29] G. Czjzek, J. Fink, F. Götz, H. Schmidt, J.M.D. Coey, J.-P. Rebouillat, A. Liénard, Phys. Rev. B 23 (1981) 2513–2530.
[30] G. Le Caër, R.A. Brand, J. Phys. Condens. Matter 10 (1998) 10715–10774.
[31] G.R. Anstis, P. Chantikul, B.R. Lawn, D.P. Marshall, J. Am. Ceram. Soc. 64 (1981) 533–538.
[32] A.R. Hanifi, A. Genson, M.J. Pomeroy, S. Hampshire, J. Am. Ceram. Soc. 95 (2012) 600–606.
[33] R.K. Brow, R.J. Kirkpatrick, G.L. Turner, J. Am. Ceram. Soc. 76 (1993) 919–928.
[34] K. Okhotnikov, B. Stevensson, M. Edén, Phys. Chem. Chem. Phys. (2013), http://dx.doi.org/10.1039/C3CP51726H, (in press).
[35] M.R. Cicconi, G. Giuli, E. Paris, P. Courtial, D.B. Dingwell, J. Non-Cryst. Solids 362 (2013) 162–168.
[36] R.D. Shannon, Acta Crystallogr. 32 (1976) 751–767.